
DiReCT: Diagnostic Reasoning for Clinical Notes via Large Language Models

**Bowen Wang^{♣◇}, Jiuyang Chang^{♡*}, Yiming Qian^{♠†}, Guoxin Chen[★], Junhao Chen[◇],
Zhouqiang Jiang[◇], Jiahao Zhang[◇], Yuta Nakashima^{◇♣}, Hajime Nagahara^{◇♣}**

[♣]Premium Research Institute for Human Metaverse Medicine (WPI-PRIME), Osaka University,

[♡]Department of Cardiology, The First Affiliated Hospital of Dalian Medical University,

[★]Institute of Computing Technology, Chinese Academy of Science

[◇]D3 Center, Osaka University, [♠]Agency for Science, Technology and Research (A*STAR),

{wang, n-yuta, nagahara}@ids.osaka-u.ac.jp

changjiuyang@firsthosp-dmu.com

qiany@ihpc.a-star.edu.sg, gx.chen.chn@gmail.com

{junhao, zhouqiang, jiahao}@is.ids.osaka-u.ac.jp

Abstract

Large language models (LLMs) have recently showcased remarkable capabilities, spanning a wide range of tasks and applications, including those in the medical domain. Models like GPT-4 excel in medical question answering but may face challenges in the lack of interpretability when handling complex tasks in real clinical settings. We thus introduce the diagnostic reasoning dataset for clinical notes (DiReCT), aiming at evaluating the reasoning ability and interpretability of LLMs compared to human doctors. It contains 511 clinical notes, each meticulously annotated by physicians, detailing the diagnostic reasoning process from observations in a clinical note to the final diagnosis. Additionally, a diagnostic knowledge graph is provided to offer essential knowledge for reasoning, which may not be covered in the training data of existing LLMs. Evaluations of leading LLMs on DiReCT bring out a significant gap between their reasoning ability and that of human doctors, highlighting the critical need for models that can reason effectively in real-world clinical scenarios [‡].

1 Introduction

Recent advancements of large language models (LLMs) [Zhao et al., 2023] have ushered in new possibilities and challenges for a wide range of natural language processing (NLP) tasks [Min et al., 2023]. In the medical domain, these models have demonstrated remarkable prowess [Anil et al., 2023, Han et al., 2023], particularly in medical question answering (QA) [Jin et al., 2021]. Leading-edge models, such as GPT-4 [OpenAI, 2023a], exhibit profound proficiency in understanding and generating text [Bubeck et al., 2023], even achieved high scores on the United States Medical Licensing Examination (USMLE) questions [Nori et al., 2023].

Despite the advancements, interpretability is critical, particularly in medical NLP tasks [Liévin et al., 2024] because these tasks directly impact patient health and treatment decisions. Without clear interpretability, there’s a risk of misdiagnosis and improper treatment, making it vital for ensuring medical safety. Some studies assess this capability over medical QA [Pal et al., 2022, Li et al., 2023,

^{*}Equal contribution.

[†]Corresponding author.

[‡]Data and code are available at <https://github.com/wbw520/DiReCT>.

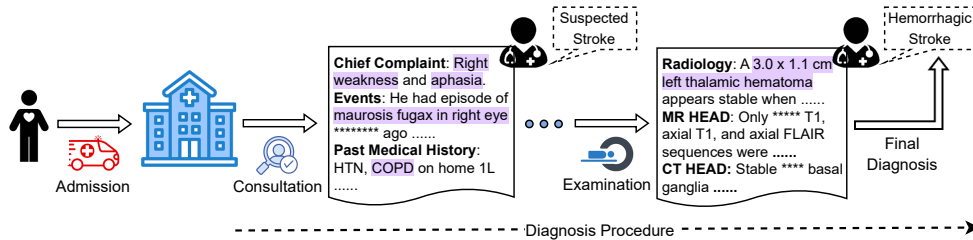


Figure 1: When a patient is admitted, an initial consultation takes place to collect subjective information. Subsequent observations may then require further examination to confirm the diagnosis.

Chen et al., 2024] or natural language inference (NLI) [Jullien et al., 2023]. Putting more attention on interpretability, they use relatively simple tasks as testbeds, taking short text as input. Nevertheless, real-world clinical tasks are often more complex [Gao et al., 2023a], as illustrated in Figure 1, a typical diagnosis requires comprehending and combining various information, such as health records, physical examinations, and laboratory tests, for further reasoning of possible diseases in a step-by-step manner following the established guidelines. This observation suggests that both *perception*, or reading (e.g., finding necessary information in the medical record) and *reasoning* (determining the disease based on the observations) should be counted when evaluating interpretability in LLM-based medical NLP tasks.

For a more comprehensive evaluation of LLMs for supporting diagnosis in a more realistic setting, we propose a **Diagnostic Reasoning** dataset for **Clinical noTies** (DiReCT). The task basically is predicting the diagnosis from a *clinical note* of a patient, which is a collection of various medical records, written in natural language. Our dataset contains 511 clinical notes spanning 25 disease categories, sampled from a publicly available database, MIMIC-IV [Johnson et al., 2023]. Each clinical note undergoes fine-grained annotation by professional physicians. The annotators (i.e., the physicians) are responsible for identifying the text, or the *observation*, in the note that leads to a certain diagnosis, as well as the explanation. The dataset also provides a diagnostic knowledge graph based on existing diagnostic guidelines to facilitate more consistent annotations and to supply a model with essential knowledge for reasoning that might not be encompassed in its training data.

To underscore the challenge offered by our dataset, we propose a simple AI-agent based baseline [Xi et al., 2023, Tang et al., 2023] that utilizes the knowledge graph to decompose the diagnosis into a sequence of diagnoses from a smaller number of observations. Our experimental findings indicate that current state-of-the-art LLMs still fall short of aligning well with human doctors.

Contribution. DiReCT offers a new challenge in diagnosis from a complex clinical note with explicit knowledge of established guidelines. This challenge aligns with a realistic medical scenario that doctors are experiencing. In the application aspect, the dataset facilitates the development of a model to support doctors in diagnosis, which is error-prone [Middleton et al., 2013, Liu et al., 2022]. From the technical aspect, the dataset can benchmark models’ ability to read long text and find necessary observations for *multi-evidence entailment tree* reasoning, an extension of the original entailment tree explanation [Dalvi et al., 2021] for complex scenarios in medical NLP tasks. As shown in Figure 3, this is not trivial because of the variations in writing; superficial matching does not help, and medical knowledge is vital. Meanwhile, reasoning itself is facilitated by the knowledge graph. The model does not necessarily have the knowledge of diagnostic guidelines. With this choice, the knowledge graph explains the reasoning process, which is also beneficial when deploying such a diagnosis assistant system in practical uses.

2 Related Works

Natural language explanation. Recent advancements in NLP have led to significant achievements [Min et al., 2023]. However, existing models often lack explainability, posing potential risks [Danilevsky et al., 2020, Gurrupu et al., 2023]. Numerous efforts have been made to address this challenge. One effective approach is to provide a human-understandable *plain text* explanation alongside the model’s output [Camburu et al., 2018, Rajani et al., 2019]. Another strategy involves identifying *evidence* within the input that serves as a rationale for the model’s decisions, aligning with

Table 1: Comparison of existing datasets for medical reasoning tasks and ours. “t” and “w” mean tokens and words for the length of input, respectively.

Dataset	Task	Data Source	Length	Explanation	# Cases
MedMCQA [Pal et al., 2022]	QA	Examination	9.93 t	Plain Text	194,000
ExplainCPE [Li et al., 2023]	QA	Examination	37.79 w	Plain Text	7,000
JAMA Challenge [Chen et al., 2024]	QA	Clinical Cases	371 w	Plain Text	1,524
Medbullets [Chen et al., 2024]	QA	Online Questions	163 w	Plain Text	308
N2N2 [Gao et al., 2022]	Sum	Clinical Notes	785.46 t	Evidences	768
NLI4CT [Jullien et al., 2023]	NLI	Clinical Trial Reports	10-35 t	Multi-hop	2,400
NEJM CPC [Zack et al., 2023]	CD	Clinical Cases	-	Plain Text	2,525
DiReCT (Ours)	CD	Clinical Notes	1074.6 t	Entailment Tree	511

human reasoning [DeYoung et al., 2020]. Expanding on this concept, [Jhamtani and Clark, 2020] introduces chain-structured explanations, given that a diagnosis can demand multi-hop reasoning. This idea is further refined by ProofWriter [Tafjord et al., 2021] through a proof stage for explanations, and by [Zhao et al., 2021] through retrieval from a corpus. [Dalvi et al., 2021] proposes the *entailment tree*, offering more detailed explanations and facilitating inspection of the model’s reasoning. More recently, [Zhang et al., 2024] employed cumulative reasoning to tap into the potential of LLMs to provide explanation via a *directed acyclic graph*. Although substantial progress has been made, interpreting NLP tasks in medical domains remains an ongoing challenge [Liévin et al., 2024].

Benchmarks of interpretability in the medical domain Several datasets are designed to assess a model’s reasoning together with its interpretability in medical NLP (Table 1). MedMCQA [Pal et al., 2022] and other medical QA datasets [Li et al., 2023, Chen et al., 2024] provide plain text as explanations for QA tasks. NLI4CT [Jullien et al., 2023] uses clinical trial reports, focusing on NLI supported by multi-hop reasoning. N2N2 [Gao et al., 2022] proposes a summarization (Sum) task for a diagnosis based on multiple pieces of evidence in the input clinical note. NEJM CPC [Zack et al., 2023] interprets clinicians’ diagnostic reasoning as plain text for reasoning clinical diagnosis (CD). DR.BENCH [Gao et al., 2023b] aggregates publicly available datasets to assess the diagnostic reasoning of LLMs. Utilizing an multi-evidence entailment tree explanation, DiReCT introduces a more rigorous task to assess whether LLMs can align with doctors’ reasoning in real clinical settings.

3 A benchmark for Clinical Notes Diagnosis

This section first detail clinical notes (Section 3.1). We also describes the knowledge graph that encodes existing guidelines (Section 3.2). Our task definition, which tasks a clinical note and the knowledge graph as input is given in Section 3.4. We then present our annotation process for clinical notes (Section 3.3) and the evaluation metrics (Section 3.5).

3.1 Clinical Notes

Clinical notes used in DiReCT are stored in the SOAP format [Weed, 1970]. A clinical note comprises four components: In the *subjective* section, the physician records the patient’s chief complaint, the history of present illness, and other subjective experiences reported by the patient. The *objective* section contains structural data obtained through examinations (inspection, auscultation, etc.) and other measurable means. The *assessment* section involves the physician’s analysis and evaluation of the patient’s condition. This may include a summary of current status, *etc.* Finally, the *plan* section outlines the physician’s proposed treatment and management plan. This may include prescribed medications, recommended therapies, and further investigations. A clinical note also includes a primary discharge diagnosis (PDD) in the assessment section.

DiReCT’s clinical notes are sourced from the MIMIC-IV dataset [Johnson et al., 2023] (PhysioNet Credentialed Health Data License 1.5.0), which encompasses over 40,000 patients admitted to the intensive care units. Each note contains clinical data for a patient. To construct DiReCT, we curated a subset of 511 notes whose PDDs fell within one of 25 disease categories i in 5 medical domains.

In our task, a note $R = \{r\}$ is an excerpt of 6 clinical data in the subjective and objective sections (i.e., $|R| = 6$): chief complaint, history of present illness, past medical history, family history, physical

exam, and pertinent results.¹ We also identified the PDD d^* associated with R .² The set of d^* 's for all R 's collectively forms \mathcal{D}^* . We manually removed any descriptions that disclose the PDD in R .

3.2 Diagnostic Knowledge Graph

Existing knowledge graphs for the medical domain, e.g., UMLS KG [Bodenreider, 2004], lack the ability to provide specific clinical decision support (e.g., diagnostic threshold, context-specific data, dosage information, etc.), which are critical for accurate diagnosis.

Our knowledge graphs $\mathcal{K} = \{k_i\}$ is a collection of graph k_i for disease category i . k_i is based on the diagnosis criteria in existing guidelines (refer to supplementary material for details). k_i 's nodes are either premise $p \in \mathcal{P}_i$ (medical statement, e.g., Headache is a symptom of) and diagnoses $d \in \mathcal{D}_i$ (e.g., Suspected Stroke). k_i consists of two different types of edges. One is *premise-to-diagnosis* edges $\mathcal{S}_i = \{(p, d)\}$; an edge is from p to d . This edge represents the necessary premise p to make a diagnosis d . We refer to them as *supporting* edges. The other is *diagnosis-to-diagnosis* edges $\mathcal{F}_i = \{(d, d')\}$, where $d, d' \in \mathcal{D}_i$ and the edge is from d to d' , which represents the diagnostic flow. These edges are referred to as *procedural* edges.

A disease category is defined according to an existing guideline, which starts from a certain diagnosis; therefore, a procedural graph $g_i = (\mathcal{D}_i, \mathcal{F}_i)$ ($\mathcal{G} = \{g_i\}$) has only one root node and arbitrarily branches toward multiple leaf nodes that represent PDDs (i.e., the clinical notes in DiReCT are chosen to cover all leaf nodes of g_i). Thus, g_i is a *tree*. We denote the set of the leaf nodes (or PDDs) as $\mathcal{D}_i^* \subset \mathcal{D}_i$. The knowledge graph is denoted by $k_i = (\mathcal{D}_i, \mathcal{P}_i, \mathcal{S}_i, \mathcal{F}_i)$.

Figure 2 shows a part of k_i , where i is Acute Coronary Syndromes (ACS). Premises in \mathcal{P}_i and diagnoses in \mathcal{D}_i are given in the blue and gray boxes, while PDDs in \mathcal{D}_i^* are ones without outgoing edges (i.e., STEMI-ACS and NSTEMI-ACS, and UA). The black and red arrows are edges in \mathcal{S} and \mathcal{F} , respectively, where the black arrows indicate the supporting edges.

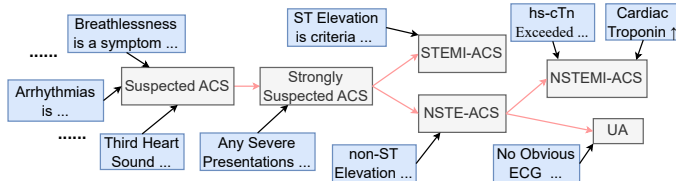


Figure 2: A part of k_i for i being Acute Coronary Syndromes.

\mathcal{K} serves two essential functions: (1) They serve as the gold standard for annotation, guiding doctors in the precise and uniform interpretation of clinical notes. (2) Our task also allows a model to use them to ensure the output from an LLM can be closely aligned with the reasoning processes of medical professionals.

3.3 Data Annotation

Let $d^* \in \mathcal{D}_i^*$ denote the PDD of disease category i associated with R . We can find a subgraph $k_i(d^*)$ of k_i that contains all ancestors of d^* , including premises in \mathcal{P}_i . We also denote the set of supporting edges in $k_i(d^*)$ as $\mathcal{S}_i(d^*)$. Our annotation process is, for each supporting edge $(p, d) \in \mathcal{S}_i(d^*)$, to extract observation $o \in \mathcal{O}$ in R (highlighted text in the clinical note in Figure 3) and provide rationalization z of this *deduction* why o is a support for d or corresponds to p .³ They form the explanation $\mathcal{E} = \{(o, z, d)\}$ for (R, d^*) . This annotation process was carried out by 9 clinical physicians and subsequently verified for accuracy and completeness by three senior medical experts.

Table 2 summarizes statistics of our dataset. The second and third columns (“# cats.” and “# samples”) show the numbers of disease categories and samples in the respective medical domains. $|\mathcal{D}_i|$ and $|\mathcal{D}_i^*|$ are the total numbers of diagnoses (diseases) and PDDs, summed over all diagnostic categories

¹We excluded data, such as review system and social history, because they are often missing in the original clinical notes and are less relevant to the diagnosis.

²All clinical notes in DiReCT are related to only one PDD, and there is no secondary discharge diagnosis.

³All annotations strictly follow the procedural flow in k_i , and each observation is only related to one diagnostic node. If R does not provide sufficient observations for the PDD (which may happen when a certain test is omitted), the annotators were asked to add plausible observations to R . Refer to amended data points in supplementary for details.

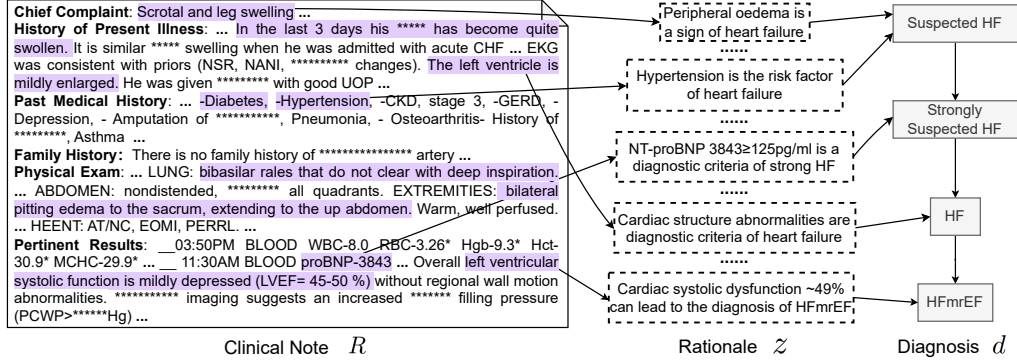


Figure 3: An annotation sample of Heart Failure (HF). The left part is the clinical note alongside extracted observations by a doctor. The middle part outlines the steps of the rationale for the premise corresponding to each diagnostic node shown in the right part.

in the medical domain, respectively. $|\mathcal{O}|$ is the average number of annotated observations. “Length” is the average number of tokens in R .

3.4 Task Definition

We propose two tasks with different levels of supplied external knowledge. The first task is, given R and \mathcal{G} , to predict the associated PDD d^* and generate an explanation \mathcal{E} that explains the model’s diagnostic procedure from R to d^* , i.e., letting M denote a model:

$$\hat{d}^*, \hat{\mathcal{E}} = M(R, \mathcal{G}), \quad (1)$$

where $\hat{d}^* \in \cup_i \mathcal{D}_i^*$ and $\hat{\mathcal{E}}$ are predictions for the PDD and explanation, respectively. With this task, the knowledge of specific diagnostic procedures in existing guidelines can be used for prediction, facilitating interpretability. The second task takes \mathcal{K} as input instead of \mathcal{G} , i.e.,:

$$\hat{d}^*, \hat{\mathcal{E}} = M(R, \mathcal{K}). \quad (2)$$

This task allows for the use of broader knowledge of premises for prediction. One may also try a task without any external knowledge.

3.5 Evaluation Metrics

We designed three metrics to quantify the predictive performance over our benchmark.

(1) *Accuracy of diagnosis* Acc^{diag} evaluates if a model can correctly identify the diagnosis. $Acc^{\text{diag}} = 1$ if $d^* = \hat{d}$, and $Acc^{\text{diag}} = 0$ otherwise. The average is reported.

(2) *Completeness of observations* Obs^{comp} evaluates whether a model extracts all and only necessary observations for the prediction. Let \mathcal{O} and $\hat{\mathcal{O}}$ denote the sets of observations in \mathcal{E} and $\hat{\mathcal{E}}$, respectively. The metric is defined as $Obs^{\text{comp}} = |\mathcal{O} \cap \hat{\mathcal{O}}| / |\mathcal{O} \cup \hat{\mathcal{O}}|$, where the numerator is the number of observations that are common in both \mathcal{O} and $\hat{\mathcal{O}}$.⁴ This metric simultaneously evaluates the correctness of each observation and the coverage. To supplement it, we also report the precision Obs^{pre} and recall Obs^{rec} , given by $Obs^{\text{pre}} = |\mathcal{O} \cap \hat{\mathcal{O}}| / |\hat{\mathcal{O}}|$ and $Obs^{\text{rec}} = |\mathcal{O} \cap \hat{\mathcal{O}}| / |\mathcal{O}|$.

(3) *Faithfulness of explanations* evaluates if the diagnostic flow toward the PDD is fully supported by observations with faithful rationalizations. This involves establishing a one-to-one correspondence between deductions in the prediction and the ground truth. We use the correspondences established for computing Obs^{comp} . Let $o \in \mathcal{O}$ and $\hat{o} \in \hat{\mathcal{O}}$ denote corresponding observations. This correspondence

⁴We find the common observations with an LLM (refer to the supplementary material for more detail).

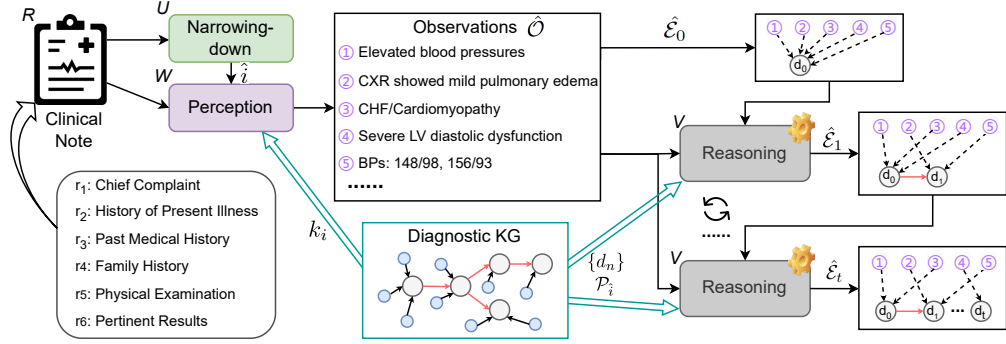


Figure 4: Pipeline of our baseline. The dotted line in the right-most boxes means deductions from an observation to a diagnosis.

is considered successful if z and \hat{z} as well as d and \hat{d} associated with o and \hat{o} matches. Let $m(\mathcal{E}, \hat{\mathcal{E}})$ denote the number of successful matches. We use the ratio of $m(\mathcal{E}, \hat{\mathcal{E}})$ to $|\mathcal{O} \cap \hat{\mathcal{O}}|$ and $|\mathcal{O} \cup \hat{\mathcal{O}}|$ as evaluation metrics Exp^{com} and Exp^{all} , respectively, to see failures come from observations or explanations and diagnosis.

4 Baseline

Figure 4 provides an overview of our baseline, which comprises three LLM-based modules: narrowing-down (U), perception (W), and reasoning (V). In our experiments, each module utilizes the same type of LLM with different prompts (refer to the supplementary material for more details). U analyze the entire note R to determine the possible disease type \hat{i} . W extracts observations that may lead to diseases from each r , producing a list of original disease descriptions. V iteratively derives possible diseases from observations based on the diagnosis knowledge graph, providing rationales for each deduction (o, z, d) .

The narrowing-down module U takes R as input to make a prediction \hat{i} of the disease category, i.e., $\hat{i} = U(R)$. Let $d_t \in \mathcal{D}_{\hat{i}}$ be the diagnosis that has been reached with t iterations over $k_{\hat{i}}$, where t corresponds to the depth of node d_t and so is less than or equal to the depth of $k_{\hat{i}}$. d_0 is the root node of $k_{\hat{i}}$. For d_0 , we apply the perception module to extract all observations in R and explanation \mathcal{E}_0 to support d_0 as

$$\hat{\mathcal{O}}, \hat{\mathcal{E}}_0 = W(d_0, k_{\hat{i}}). \quad (3)$$

$k_{\hat{i}}$ is supplied to facilitate the model to extract all observations for the following reasoning process.⁵ After the perception module W (iteration $t = 0$), we obtain all observations $\hat{\mathcal{O}}$, the root node of the diagnosis d_0 , and an explanation $\hat{\mathcal{E}}_0$ for the initial iteration. Assuming that by iteration t , we already know the diagnosis for iteration t as d_t . $\{d_n\}$ is the set of d_t 's children, and $\mathcal{P}_{\hat{i}}(\{d_n\})$ represents the corresponding premises that support each d_n . V identifies the diagnosis for the next step, d_{t+1} , and provides a justification \mathcal{E}_{t+1} . V will verify if there is any \hat{o} in $\hat{\mathcal{O}}$ that supports a d_n . If fully supported, d_n is identified as d_{t+1} for the $(t + 1)$ -th iteration, i.e.,

$$d_{t+1}, \hat{\mathcal{E}}_{t+1} = V(\hat{\mathcal{O}}, \{d_n\}, \mathcal{P}_{\hat{i}}(\{d_n\})), \quad (4)$$

V continues until d_{t+1} in \mathcal{D}^* is identified. If no observation supports a d_n , the reasoning process will be stopped.

In our annotation, an observation o is associated with only one d . However, our method employs an iterative reasoning pipeline. Initially, the perception module W generates an explanation set $\hat{\mathcal{E}}_0$, linking all \hat{o} to d_0 . During the t -th iteration of V , the explanation set is $\hat{\mathcal{E}}_t$, where at least one \hat{o} is

⁵We used only pairs of an observation and a premise. We abuse \mathcal{K} to mean this for notation simplicity. The perception model can also utilize g_i instead of k_i for the first task.

Table 3: Evaluation of diagnostic reasoning ability using \mathcal{G} or \mathcal{K} as input.

Task	Models	Diagnosis		Observation			Explanation	
		Acc^{cat}	Acc^{diag}	Obs^{pre}	Obs^{rec}	Obs^{comp}	Exp^{com}	Exp^{all}
With \mathcal{G}	Zephyr 7B	0.274	0.151	0.123 \pm 0.200	0.115 \pm 0.166	0.092 \pm 0.108	0.071 \pm 0.139	0.014 \pm 0.037
	Mistral 7B	0.507	0.306	0.211 \pm 0.190	0.317 \pm 0.253	0.173 \pm 0.157	0.230 \pm 0.312	0.062 \pm 0.088
	Mixtral 8 \times 7B	0.413	0.237	0.147 \pm 0.165	0.266 \pm 0.261	0.124 \pm 0.138	0.144 \pm 0.268	0.029 \pm 0.056
	LLama3 8B	0.569	0.364	0.248 \pm 0.157	0.410 \pm 0.218	0.211 \pm 0.138	0.325 \pm 0.375	0.087 \pm 0.118
	LLama3 70B	0.822	0.606	0.306 \pm 0.151	0.543\pm0.183	0.279 \pm 0.146	0.409 \pm 0.328	0.124 \pm 0.120
	GPT-3.5 turbo	0.679	0.455	0.389 \pm 0.212	0.351 \pm 0.192	0.275 \pm 0.167	0.331 \pm 0.366	0.103 \pm 0.127
GPT-4 turbo	0.804	0.610	0.486\pm0.207	0.481 \pm 0.180	0.391\pm0.189	0.481\pm0.362	0.210\pm0.188	
With \mathcal{K}	LLama3 8B	0.576	0.344	0.235 \pm 0.162	0.394 \pm 0.227	0.199 \pm 0.142	0.327 \pm 0.375	0.087 \pm 0.114
	LLama3 70B	0.786	0.652	0.268 \pm 0.147	0.524\pm0.211	0.258 \pm 0.142	0.549 \pm 0.372	0.152 \pm 0.130
	GPT-3.5 turbo	0.652	0.413	0.347 \pm 0.241	0.279 \pm 0.203	0.232 \pm 0.184	0.374 \pm 0.408	0.121 \pm 0.152
	GPT-4 turbo	0.808	0.611	0.470\pm0.209	0.459 \pm 0.190	0.371\pm0.192	0.645\pm0.385	0.273\pm0.216

linked to d_t . The final diagnosis explanation is the combination of $\hat{\mathcal{E}}_0, \dots, \hat{\mathcal{E}}_T$ and d_0, \dots, d_T , where T represents the final iteration. In this combination, if an \hat{o} is eventually processed in the iteration for $\hat{\mathcal{E}}_t$, the corresponding (o, z, d) in all preceding $\hat{\mathcal{E}}_0, \dots, \hat{\mathcal{E}}_{t-1}$ will be removed. That is, \hat{o} will always be possessed by the d_t closest to the leaf PDD node.

5 Experiments

5.1 Experimental Setup

We assess the reasoning capabilities of 7 recent LLMs from diverse families and model sizes, including 5 instruction-tuned models that are openly accessible: LLama3 8B and 70B [AI@Meta, 2024], Zephyr 7B [Tunstall et al., 2023], Mistral 7B [Jiang et al., 2023], and Mixtral 8 \times 7B [Jiang et al., 2023]. We have also obtained access to private versions of the GPT-3.5 turbo [OpenAI, 2023b] and GPT-4 turbo [OpenAI, 2023a]⁶, which are high-performance closed-source models. Each LLM is utilized to implement our baseline’s narrowing-down, perception, and reasoning modules. The temperature is set to 0. For computing evaluation metrics, we use LLama3 8B with few-shot prompts to make correspondences between \mathcal{O} and $\hat{\mathcal{O}}$ as well as to verify a match between predicted and ground-truth explanations (refer to the supplementary material for more details).

5.2 Results

Comparison among LLMs. Table 3 shows the performance of our baseline built on top of various LLMs. We first evaluate a variant of our task that takes graph $\mathcal{G} = \{\mathcal{G}_i\}$ consisting of only procedural flow as external knowledge instead of \mathcal{K} . Comparison between \mathcal{G} and \mathcal{K} demonstrates the importance of supplying premises with the model and LLMs’ capability to make use of extensive external knowledge that may be superficially different from statements in R . Subsequently, some models are evaluated with our task using \mathcal{K} . In addition to the metrics in Section 3.5, we also adopt the *accuracy of disease category* Acc^{cat} , which gives 1 when $\hat{i} = i$, as our baseline’s performance depends on it.

With \mathcal{G} , we can see that GPT-4 achieves the best performance in most metrics, especially related to observations and explanations, surpassing LLama3 70B by a large margin. In terms of accuracy (in both category and diagnosis levels), LLama3 70B is comparable to GPT-4. LLama3 70B also has a higher Obs^{rec} but low Obs^{pre} and Obs^{comp} , which means that this model tends to extract many observations. Models with high diagnostic accuracy are not necessarily excel in finding essential information in long text (i.e., observations) and generating reasons (i.e., explanations).

When \mathcal{K} is given, all models show better diagnostic accuracy (in LLama3 70B) and explanations, while observations are slightly degraded (this may related to the instruction following ability due to the input length when giving \mathcal{K} as input). GPT-4 with \mathcal{K} enhances Acc^{diag} , Exp^{com} , and Exp^{all} scores. This suggests that premises and supporting edges are beneficial for diagnosis and explanation. Lower

⁶These two models are housed on a HIPPA-compliant instance within Microsoft Azure AI Studio. No data is transferred to either Microsoft or OpenAI. This secure environment enables us to safely conduct experiments with the MIMIC-IV dataset, in compliance with the Data Use Agreement.

Table 4: Evaluation of diagnostic reasoning ability without external knowledge.

Task	Models	Acc^{diag}	Observation			Explanation	
			Obs^{pre}	Obs^{rec}	Obs^{comp}	Exp^{com}	Exp^{all}
With \mathcal{D}^*	LLama3 8B	0.070	0.154 \pm 0.139	0.330 \pm 0.244	0.135 \pm 0.122	0.020 \pm 0.100	0.004 \pm 0.016
	LLama3 70B	0.502	0.257 \pm 0.150	0.509\pm0.213	0.237 \pm 0.145	0.138 \pm 0.209	0.034 \pm 0.054
	GPT-3.5 turbo	0.223	0.164 \pm 0.242	0.149 \pm 0.212	0.116 \pm 0.174	0.091 \pm 0.231	0.025 \pm 0.065
	GPT-4 turbo	0.636	0.461\pm0.206	0.482 \pm 0.160	0.378\pm0.174	0.186\pm0.221	0.074\pm0.090
No Knowledge	LLama3 8B	0.023	0.137 \pm 0.159	0.258 \pm 0.274	0.119 \pm 0.141	0.018 \pm 0.083	0.006 \pm 0.026
	LLama3 70B	0.037	0.246 \pm 0.148	0.504\pm0.222	0.227 \pm 0.148	0.022 \pm 0.093	0.007 \pm 0.030
	GPT-3.5 turbo	0.059	0.161 \pm 0.238	0.148 \pm 0.215	0.113 \pm 0.171	0.036 \pm 0.131	0.011 \pm 0.039
	GPT-4 turbo	0.074	0.410\pm0.208	0.443 \pm 0.191	0.324\pm0.182	0.047\pm0.143	0.019\pm0.058

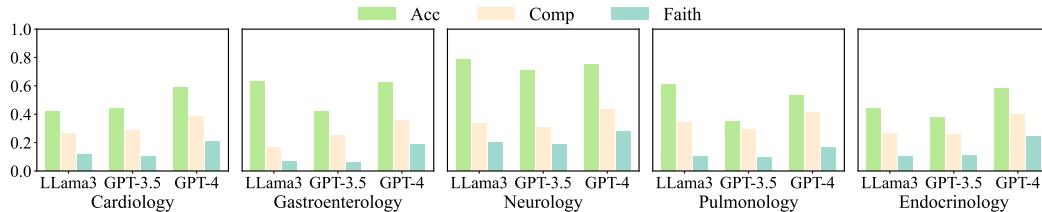


Figure 5: Performance of LLaMa3 70B, GPT-3.5, and GPT-4 under different medical domains. We use the task with \mathcal{G} .

observational performance may indicate that the models lack the ability to associate premises and text in R , which are often superficially different though semantically consistent.

LLMs may undergo inherent challenges for evaluation when no external knowledge is supplied. They may have the knowledge to diagnose but cannot make consistent observations and explanations that our task expects through \mathcal{K} . To explore this, we evaluate two settings: (1) giving \mathcal{D}^* and (2) no knowledge is supplied to a model (shown in Table 4). The prompts used for this setup are detailed in the supplementary material. We do not evaluate the accuracy of disease category prediction as it is basically the same as Table 3. We can clearly see that with \mathcal{D}^* , GPT-4’s diagnostic and observational scores are comparable to those of the task with \mathcal{K} , though explanatory performance is much worse. Without any external knowledge, the diagnostic accuracy is also inferior.⁷ The deteriorated performance can be attributed to inconsistent wording of diagnosis names, which makes evaluation tough. High observational scores imply that observations in R can be identified without relying on external knowledge. There can be some cues to spot them.

Performance in individual domains. Figure 5 summarizes the performance of LLaMa3 70B, GPT-3.5, and GPT-4 across different medical domains, evaluated using Acc^{diag} , Obs^{comp} (Comp), and Exp^{all} (Faith). Neurology gives the best diagnostic accuracy, where LLaMa3 achieved an accuracy of 0.779. GPT-4 also performed well (0.753). In terms of Obs^{comp} and Exp^{all} , GPT-4’s results were 0.437 and 0.280, respectively. However, GPT-4 yields a higher diagnostic accuracy score while a lower explanatory score, suggesting that the observations captured by the model or their rationalizations differ from human doctors.

Diagnostic reasoning under conditions of incomplete observation. In real-world scenarios, doctors often have to make diagnoses based on incomplete information. To explore this, we conducted experiments on the 73 amended cases which originally lack observation to the final diagnosis (refer to supplementary for detailed introduction of amended data point). One set of experiments used the unmodified original notes, labeled as "Original," while the other set used notes with added observations labeled as "Amended." We tested three models—Llama3 70B, GPT-3.5-turbo, and GPT-4 turbo—under two settings: one with only the procedural graph \mathcal{G} and the other with the complete knowledge graph \mathcal{K} . The results are presented in Tables 5 and 6. We can observe that in both \mathcal{G} and \mathcal{K} settings, the performance on the Amended data was consistently better across all metrics compared to the Original data. This suggests that even a single added observation can significantly impact the model’s diagnostic reasoning.

⁷We understand this comparison is unfair, as the prompts differ. We intend to give a rough idea about the challenge without external knowledge.

Table 5: Amendment ablation study using \mathcal{G} .

Setting	Models	Diagnosis		Observation			Explanation	
		Acc^{cat}	Acc^{diag}	Obs^{pre}	Obs^{rec}	Obs^{comp}	Exp^{com}	Exp^{all}
Original	LLama3 70B	0.547	0.273	0.225 \pm 0.143	0.472 \pm 0.144	0.253 \pm 0.138	0.216 \pm 0.271	0.073 \pm 0.087
	GPT-3.5 turbo	0.507	0.273	0.393 \pm 0.216	0.355 \pm 0.174	0.278 \pm 0.151	0.207 \pm 0.305	0.062 \pm 0.093
	GPT-4 turbo	0.616	0.328	0.446 \pm 0.211	0.418 \pm 0.164	0.340 \pm 0.178	0.242 \pm 0.324	0.098 \pm 0.137
Amended	LLama3 70B	0.698	0.534	0.250 \pm 0.173	0.507 \pm 0.134	0.240 \pm 0.129	0.296 \pm 0.354	0.133 \pm 0.142
	GPT-3.5 turbo	0.671	0.411	0.487 \pm 0.206	0.351 \pm 0.152	0.310 \pm 0.145	0.272 \pm 0.321	0.092 \pm 0.118
	GPT-4 turbo	0.726	0.547	0.546 \pm 0.184	0.465 \pm 0.148	0.412 \pm 0.171	0.391 \pm 0.374	0.180 \pm 0.186

Table 6: Amendment ablation study using \mathcal{K} .

Setting	Models	Diagnosis		Observation			Explanation	
		Acc^{cat}	Acc^{diag}	Obs^{pre}	Obs^{rec}	Obs^{comp}	Exp^{com}	Exp^{all}
Original	LLama3 70B	0.575	0.219	0.109 \pm 0.233	0.443 \pm 0.171	0.203 \pm 0.186	0.304 \pm 0.388	0.114 \pm 0.135
	GPT-3.5 turbo	0.548	0.233	0.293 \pm 0.243	0.218 \pm 0.198	0.184 \pm 0.166	0.251 \pm 0.357	0.072 \pm 0.106
	GPT-4 turbo	0.616	0.260	0.452 \pm 0.241	0.410 \pm 0.211	0.349 \pm 0.223	0.467 \pm 0.437	0.220 \pm 0.256
Amended	LLama3 70B	0.685	0.537	0.261 \pm 0.195	0.493 \pm 0.230	0.277 \pm 0.171	0.452 \pm 0.407	0.185 \pm 0.194
	GPT-3.5 turbo	0.657	0.465	0.390 \pm 0.227	0.272 \pm 0.194	0.232 \pm 0.156	0.401 \pm 0.394	0.127 \pm 0.145
	GPT-4 turbo	0.712	0.589	0.534 \pm 0.214	0.452 \pm 0.180	0.401 \pm 0.201	0.607 \pm 0.442	0.286 \pm 0.258

For Cardiology and Endocrinology, the diagnostic accuracy of the models is relatively low (GPT-4 achieved 0.458 and 0.468, respectively). Nevertheless, Obs^{comp} and Exp^{all} are relatively high. Endocrinology results in lower diagnostic accuracy and higher explanatory performance. A smaller gap may imply that in these two domains, successful predictions are associated with observations similar to those of human doctors, and the reasoning process may be analogous. Conversely, in Gastroenterology, higher Acc^{cat} is accompanied by lower Obs^{comp} and Exp^{all} (especially for LLama3), potentially indicating a significant divergence in the reasoning process from human doctors. Overall, DiReCT demonstrates that the degree of alignment between the model’s diagnostic reasoning ability and that of human doctors varies across different medical domains.

Reliability of automatic evaluation. We randomly pick out 100 samples from DiReCT and their prediction by GPT-4 over the task with \mathcal{G} to assess the consistency of our automated metrics to evaluate the observational and explanatory performance in Section 3.3 to human judgments. Three physicians joined this experiment. For each prediction $\hat{o} \in \hat{\mathcal{O}}$, they are asked to find a similar observation in ground truth \mathcal{O} . For explanatory metrics, they verify if each prediction $\hat{z} \in \hat{\mathcal{E}}$ for $\hat{o} \in \hat{\mathcal{O}}$ align with ground-truth $z \in \mathcal{E}$ corresponding to o . A prediction and a ground truth are deemed aligned for both assessments if at least

two specialists agree. We compare LLama3’s and GPT-4’s judgments to explore if there is a gap between these LLMs. As summarized in Table 7, GPT-4 achieves the best results, with LLama3 8B also displaying a similar performance. From these results, we argue that our automated evaluation metrics are consistent with human judgments, and LLama3 is sufficient for this evaluation, allowing the cost-efficient option. Detailed analysis is available in the supplementary material.

Prediction examples. Figure 6 shows a sample generated by GPT-4. The ground-truth PDD of the input clinical note is Hemorrhagic Stroke. In this figure, purple, orange, and red indicate explanations only in the ground truth, only in prediction, and common in both, respectively; therefore, red is a successful prediction of an explanation, while purple and orange are a false negative and false positive. GPT-4 treats the observation of aurosis fugax as the criteria for diagnosing Ischemic Stroke. However, this observation only supports Suspected Stroke. Conversely, observation thalamic hematoma, which is the key indicator of Hemorrhagic Stroke, is regarded as a less important clue. Such observation-diagnosis correspondence errors lead to the model’s misdiagnosis. In Figure 7, we can observe that GPT-4 can find the key observation for the diagnosis of GERD,

Table 7: Consistency of automated evaluation with human judgments. Evaluated by mean and confidence interval (CI).

Model	Observation		Rationalization	
	Mean	95% CI	Mean	95% CI
LLama3 8B	0.887	0.844 ~ 0.878	0.835	0.759 ~ 0.818
GPT-4 turbo	0.902	0.830 ~ 0.863	0.876	0.798 ~ 0.853

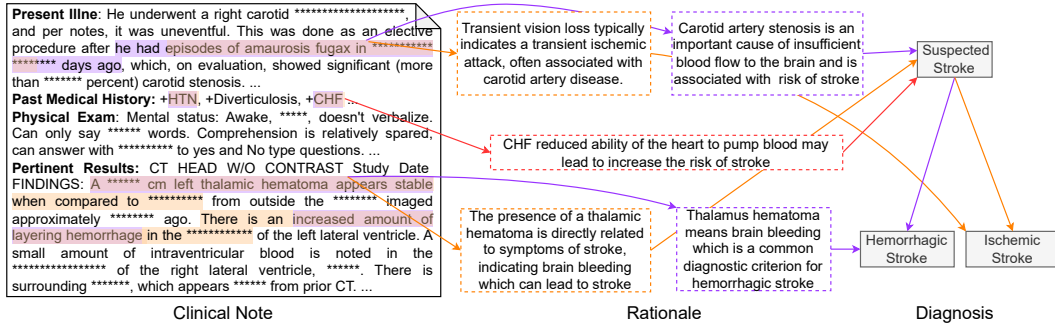


Figure 6: An example prediction for a clinical note with PDD of Hemorrhagic Stroke by GPT-4.

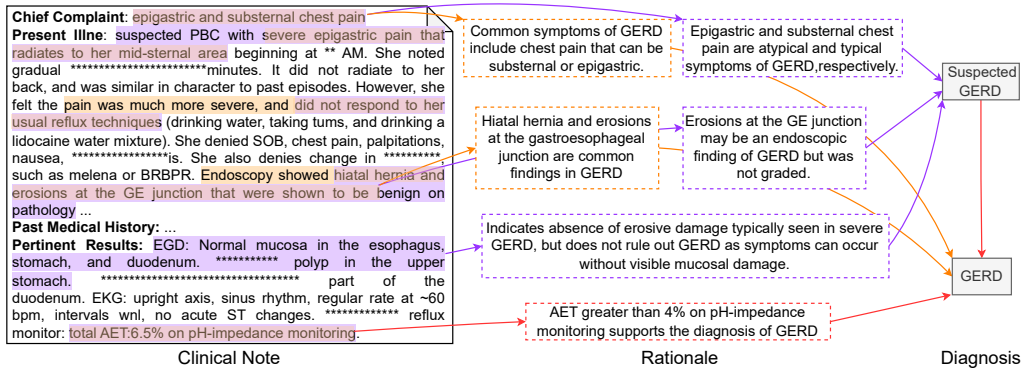


Figure 7: An example prediction for a clinical note with PDD of GERD by GPT-4

which is consistent with human in both observation and rationale. However, it still lacks the ability to identify all observations. More samples are available in the supplementary material.

6 Conclusion and Limitations

We proposed DiReCT as the first benchmark for evaluating the diagnostic reasoning ability of LLMs with interpretability by supplying external knowledge as a graph. Our evaluations reveal a notable disparity between current leading-edge LLMs and human experts, underscoring the urgent need for AI models that can perform reliable and interpretable reasoning in clinical environments. DiReCT can be easily extended to more challenging settings by removing the knowledge graph from the input, facilitating evaluations of future LLMs.

Limitations. DiReCT encompasses only a subset of disease categories and considers only one PDD, omitting the inter-diagnostic relationships due to their complexity—a significant challenge even for human doctors. Additionally, our baseline may not use optimal prompts or address issues related to hallucinations in task responses. Our dataset is solely intended for model evaluation but not for use in clinical environments. The use of the diagnostic knowledge graph is also limited to serving merely as a part of the input and once a knowledge graph is provided, the focus shifts to whether the LLM follows the graph’s rules well (refer to supplementary). Future work will focus on constructing a more comprehensive disease dataset and developing an extensive diagnostic knowledge graph.

Acknowledgments and Disclosure of Funding

This work was supported by World Premier International Research Center Initiative (WPI), MEXT, Japan. This work is also supported by JST ACT-X Grant Number JPMJAX24C8, JSPS KAKENHI No. 24K20795 and No. JP23H00497, CREST Grant No. JPMJCR20D3, JST FOREST Grant No. JPMJFR216O, and Dalian Haichuang Project for Advanced Talents.

References

- Wayne Xin Zhao, Kun Zhou, Junyi Li, Tianyi Tang, Xiaolei Wang, Yupeng Hou, Yingqian Min, Beichen Zhang, Junjie Zhang, Zican Dong, Yifan Du, Chen Yang, Yushuo Chen, Zhipeng Chen, Jinhao Jiang, Ruiyang Ren, Yifan Li, Xinyu Tang, Zikang Liu, Peiyu Liu, Jian-Yun Nie, and Ji-Rong Wen. A survey of large language models. *arXiv preprint arXiv:2303.18223*, 2023.
- Bonan Min, Hayley Ross, Elior Sulem, Amir Pouran Ben Veyseh, Thien Huu Nguyen, Oscar Sainz, Eneko Agirre, Ilana Heintz, and Dan Roth. Recent advances in natural language processing via large pre-trained language models: A survey. *ACM Computing Surveys*, 56(2):1–40, 2023.
- Rohan Anil, Andrew M Dai, Orhan Firat, Melvin Johnson, Dmitry Lepikhin, Alexandre Passos, Siamak Shakeri, Emanuel Taropa, Paige Bailey, Zhifeng Chen, et al. Palm 2 technical report. *arXiv preprint arXiv:2305.10403*, 2023.
- Tianyu Han, Lisa C Adams, Jens-Michalis Papaioannou, Paul Grundmann, Tom Oberhauser, Alexander Löser, Daniel Truhn, and Keno K Bressen. Medalpaca—an open-source collection of medical conversational ai models and training data. *arXiv preprint arXiv:2304.08247*, 2023.
- Di Jin, Eileen Pan, Nassim Oufattole, Wei-Hung Weng, Hanyi Fang, and Peter Szolovits. What disease does this patient have? a large-scale open domain question answering dataset from medical exams. *Applied Sciences*, 11(14):6421, 2021.
- OpenAI. GPT-4 Technical Report. *CoRR*, abs/2303.08774, 2023a. doi: 10.48550/arXiv.2303.08774. URL <https://doi.org/10.48550/arXiv.2303.08774>.
- Sébastien Bubeck, Varun Chandrasekaran, Ronen Eldan, Johannes Gehrke, Eric Horvitz, Ece Kamar, Peter Lee, Yin Tat Lee, Yuanzhi Li, Scott Lundberg, et al. Sparks of artificial general intelligence: Early experiments with gpt-4. *arXiv preprint arXiv:2303.12712*, 2023.
- Harsha Nori, Nicholas King, Scott Mayer McKinney, Dean Carignan, and Eric Horvitz. Capabilities of gpt-4 on medical challenge problems. *arXiv preprint arXiv:2303.13375*, 2023.
- Valentin Liévin, Christoffer Egeberg Hother, Andreas Geert Motzfeldt, and Ole Winther. Can large language models reason about medical questions? *Patterns*, 5(3), 2024.
- Ankit Pal, Logesh Kumar Umapathi, and Malaikannan Sankarasubbu. MedMCQA: A large-scale multi-subject multi-choice dataset for medical domain question answering. In *Conference on health, inference, and learning*, pages 248–260. PMLR, 2022.
- Dongfang Li, Jindi Yu, Baotian Hu, Zhenran Xu, and Min Zhang. ExplainCPE: A free-text explanation benchmark of chinese pharmacist examination. *arXiv preprint arXiv:2305.12945*, 2023.
- Hanjie Chen, Zhouxiang Fang, Yash Singla, and Mark Dredze. Benchmarking large language models on answering and explaining challenging medical questions. *arXiv preprint arXiv:2402.18060*, 2024.
- Mael Jullien, Marco Valentino, Hannah Frost, Paul O’Regan, Donal Landers, and André Freitas. Semeval-2023 task 7: Multi-evidence natural language inference for clinical trial data. *arXiv preprint arXiv:2305.02993*, 2023.
- Yanjun Gao, Ruizhe Li, John Caskey, Dmitriy Dligach, Timothy Miller, Matthew M Churpek, and Majid Afshar. Leveraging a medical knowledge graph into large language models for diagnosis prediction. *arXiv preprint arXiv:2308.14321*, 2023a.
- Alistair E. W. Johnson, Lucas Bulgarelli, Lu Shen, Alvin Gayles, Ayad Shammout, Steven Horng, Tom J. Pollard, Sicheng Hao, Benjamin Moody, Brian Gow, Li-wei H. Lehman, Leo A. Celi, and Roger G. Mark. MIMIC-IV, a freely accessible electronic health record dataset. *Scientific data*, 10(1):1, 2023.
- Zhiheng Xi, Wenxiang Chen, Xin Guo, Wei He, Yiwen Ding, Boyang Hong, Ming Zhang, Junzhe Wang, Senjie Jin, Enyu Zhou, Rui Zheng, Xiaoran Fan, Xiao Wang, Limao Xiong, Yuhao Zhou, Weiran Wang, Changhao Jiang, Yicheng Zou, Xiangyang Liu, Zhangyue Yin, Shihan Dou, Rongxiang Weng, Wensen Cheng, Qi Zhang, Wenjuan Qin, Yongyan Zheng, Xipeng Qiu, Xuanjing Huang, and Tao Gui. The rise and potential of large language model based agents: A survey, 2023.

- Xiangru Tang, Anni Zou, Zhuosheng Zhang, Yilun Zhao, Xingyao Zhang, Arman Cohan, and Mark Gerstein. Medagents: Large language models as collaborators for zero-shot medical reasoning. *arXiv preprint arXiv:2311.10537*, 2023.
- Blackford Middleton, Meryl Bloomrosen, Mark A Dente, Bill Hashmat, Ross Koppel, J Marc Overhage, Thomas H Payne, S Trent Rosenbloom, Charlotte Weaver, and Jiajie Zhang. Enhancing patient safety and quality of care by improving the usability of electronic health record systems: recommendations from amia. *Journal of the American Medical Informatics Association*, 20(e1): e2–e8, 2013.
- Jinghui Liu, Daniel Capurro, Anthony Nguyen, and Karin Verspoor. “note bloat” impacts deep learning-based nlp models for clinical prediction tasks. *Journal of biomedical informatics*, 133: 104149, 2022.
- Bhavana Dalvi, Peter Jansen, Oyvind Tafjord, Zhengnan Xie, Hannah Smith, Leighanna Papatankura, and Peter Clark. Explaining answers with entailment trees. In *Proceedings of the 2021 Conference on Empirical Methods in Natural Language Processing*, pages 7358–7370, 2021.
- Marina Danilevsky, Kun Qian, Ranit Aharonov, Yannis Katsis, Ban Kawas, and Prithviraj Sen. A survey of the state of explainable AI for natural language processing. In *Proceedings of the 1st Conference of the Asia-Pacific Chapter of the Association for Computational Linguistics and the 10th International Joint Conference on Natural Language Processing*, pages 447–459, 2020.
- Sai Gurrapu, Ajay Kulkarni, Lifu Huang, Ismini Lourentzou, and Feras A Batarseh. Rationalization for explainable nlp: A survey. *Frontiers in Artificial Intelligence*, 6, 2023.
- Oana-Maria Camburu, Tim Rocktäschel, Thomas Lukasiewicz, and Phil Blunsom. e-snli: Natural language inference with natural language explanations. *Advances in Neural Information Processing Systems*, 31, 2018.
- Nazneen Fatema Rajani, Bryan McCann, Caiming Xiong, and Richard Socher. Explain yourself! leveraging language models for commonsense reasoning. In *Proceedings of the 57th Annual Meeting of the Association for Computational Linguistics*, pages 4932–4942, Florence, Italy, 2019.
- Jay DeYoung, Sarthak Jain, Nazneen Fatema Rajani, Eric Lehman, Caiming Xiong, Richard Socher, and Byron C. Wallace. ERASER: A benchmark to evaluate rationalized NLP models. In *Proceedings of the 58th Annual Meeting of the Association for Computational Linguistics*, pages 4443–4458, 2020.
- Harsh Jhamtani and Peter Clark. Learning to explain: Datasets and models for identifying valid reasoning chains in multihop question-answering. In *Proceedings of the 2020 Conference on Empirical Methods in Natural Language Processing*, page 137–150, 2020.
- Oyvind Tafjord, Bhavana Dalvi Mishra, and Peter Clark. Proofwriter: Generating implications, proofs, and abductive statements over natural language. In *Findings of the Association for Computational Linguistics: ACL-IJCNLP*, page 3621–3634, 2021.
- Chen Zhao, Chenyan Xiong, Jordan Boyd-Graber, and Hal Daumé III. Multi-step reasoning over unstructured text with beam dense retrieval. In *Proceedings of the 2021 Conference of the North American Chapter of the Association for Computational Linguistics: Human Language Technologies*, pages 4635–4641, 2021.
- Yifan Zhang, Jingqin Yang, Yang Yuan, and Andrew Chi-Chih Yao. Cumulative reasoning with large language models. In *ICLR 2024 Workshop on Bridging the Gap Between Practice and Theory in Deep Learning*, 2024. URL <https://openreview.net/forum?id=XAAYyRxTlQ>.
- Yanjun Gao, Dmitriy Dligach, Timothy Miller, Samuel Tesch, Ryan Laffin, Matthew M. Churpek, and Majid Afshar. Hierarchical annotation for building a suite of clinical natural language processing tasks: Progress note understanding. In *Proceedings of the Thirteenth Language Resources and Evaluation Conference*, pages 5484–5493, Marseille, France, 2022. European Language Resources Association.

- Travis Zack, Gurpreet Dhaliwal, Rabih Geha, Mary Margaretten, Sara Murray, and Julian C Hong. A clinical reasoning-encoded case library developed through natural language processing. *Journal of General Internal Medicine*, 38(1):5–11, 2023.
- YanJun Gao, Dmitriy Dligach, Timothy Miller, John Caskey, Brihat Sharma, Matthew M Churpek, and Majid Afshar. Dr. bench: Diagnostic reasoning benchmark for clinical natural language processing. *Journal of Biomedical Informatics*, 138:104286, 2023b.
- L.L. Weed. *Medical Records, Medical Education, and Patient Care: The Problem-oriented Record as a Basic Tool*. Press of Case Western Reserve University, 1970. ISBN 9780815191889.
- Olivier Bodenreider. The unified medical language system (umls): integrating biomedical terminology. *Nucleic acids research*, 32(suppl_1):D267–D270, 2004.
- AI@Meta. Llama 3 model card. 2024. URL https://github.com/meta-llama/llama3/blob/main/MODEL_CARD.md.
- Lewis Tunstall, Edward Beeching, Nathan Lambert, Nazneen Rajani, Kashif Rasul, Younes Belkada, Shengyi Huang, Leandro von Werra, Clémentine Fourrier, Nathan Habib, et al. Zephyr: Direct distillation of lm alignment. *arXiv preprint arXiv:2310.16944*, 2023.
- Albert Q Jiang, Alexandre Sablayrolles, Arthur Mensch, Chris Bamford, Devendra Singh Chaplot, Diego de las Casas, Florian Bressand, Gianna Lengyel, Guillaume Lample, Lucile Saulnier, et al. Mistral 7b. *arXiv preprint arXiv:2310.06825*, 2023.
- OpenAI. Introducing ChatGPT and Whisper APIs. 2023b. URL <https://openai.com/blog/introducing-chatgpt-and-whisper-apis>.